energy&fuels

pubs.acs.org/EF Article

Realization of a Novel Free-Piston Engine Generator for Hybrid-Electric Vehicle Applications

Andrew Smallbone,* Mohd Razali Hanipah, Boru Jia, Tim Scott, Jonathan Heslop, Ben Towell, Christopher Lawrence, Sumit Roy, K. V. Shivaprasad, and Antony Paul Roskilly

Cite This: https://dx.doi.org/10.1021/acs.energyfuels.0c01647

Read Online

ACCESS | Metrics & More | Article Recommendations

ABSTRACT: Free-piston engine generators (FPEGs) have huge potential to be the principal energy conversion device for generating electricity from fuel as part of a hybrid-electric vehicle (EV) powertrain system. The principal advantages lay in the fact that they are theoretically more efficient, more compact, and more lightweight compared to other competing EV hybrid and range-extender solutions (internal combustion engines, rotary engines, fuel cells, etc.). However, this potential has yet to be realized. This article details a novel dual-piston FPEG configuration and presents the full layout of a system and provides technical evidence of a commercial FPEG system's likely size and weight. The work also presents the first results obtained from a project which set-out to realize an operational FPEG system in hardware through the development and testing of a flexible prototype test platform. The work presents the performance and control system characteristics, for a first of a kind system; these show great technical potential with stable and repeatable combustion events achieved with around 700 W per cylinder and 26% indicated efficiency.

1. INTRODUCTION

1.1. Background. The major challenges associated with electric vehicles (EVs) are their limited range and the length of time required to refuel the vehicle, both of these are limitations associated with modern electrochemical batteries. To overcome this issue, there is an opportunity to install a small on-board electric generator such that the battery can be charged during a journey—a so-called "range extender" or more simply a "hybrid-electric powertrain." These help in increasing the efficiency as well as the reliability of the system. One such advancement and the focus of this article is a free-piston engine (FPE).

As presented by Mikalsen, et al.,[1] the free-piston engine is similar to a conventional reciprocating combustion engine but with the crankshaft system replaced by a linear piston assembly, this means that the whole system can operate freely and only in a linear motion.

From the 1930s to 1960s, FPEs were used extensively as air compressors and gas generators as they offered notable advantages over conventional combustion engines, gas turbines,[2] electric generators, hydraulic pumps, and air compressors.[3] This research article presents the concept of an FPE coupled directly with a linear electric generator (known hereon as a free-piston engine generator, FPEG). The potential of this system is investigated with the overarching design objective of being used as part of a hybrid-electric vehicle power system for automotive or heavy duty transport applications or even combined heat and power (CHP) systems. Increasing research and development interest and investment into this technology has yielded an even greater numbers of FPEG prototype design configurations[4] loosely based on the FPEG concept itself. As presented in Jia, et al.,[5] these can in general be categorized into four main types of engine as opposed-piston two-stroke, opposed-piston four-stroke, single-piston two-stroke, and dual-piston two-stroke. The following provides a summary of the current status of the technology based on these categories and specifically focus on those which have been realized with reported performance data.

1.2. Literature Review. Numerous modeling studies have been conducted to explore the potential of FPEGs.[6−10] However, the following is a description of the experimental investigations that typically have different configurations and combustion modes to that presented in the present work.

The technical opportunity for fuel cells, supercapacitors, and FPEG have been explored by researchers at the German Aerospace Center (GAC),[11,12] who concluded that FPEG are favorable in terms of cost and overall efficiency. The GAC team developed a FPEG prototype system,[13] which was comprised of three main subsystems: (1) a linear generator, (2) a gas spring bounce, and (3) a cylinder/piston assembly designed to operate as an internal combustion engine (ICE). The engine[14] had four-cylinder head mounted valves and was designed to operate in two-stroke mode. To achieve high compression ratios, the top dead volume of the cylinder was minimized and the stroke kept short. Operating at 21 Hz, the GAC team reported[13] that top dead center (TDC) was at 57.5% of the periodic time yielding 10 kW_e.

Received: May 22, 2020
Revised: September 3, 2020
Published: September 7, 2020

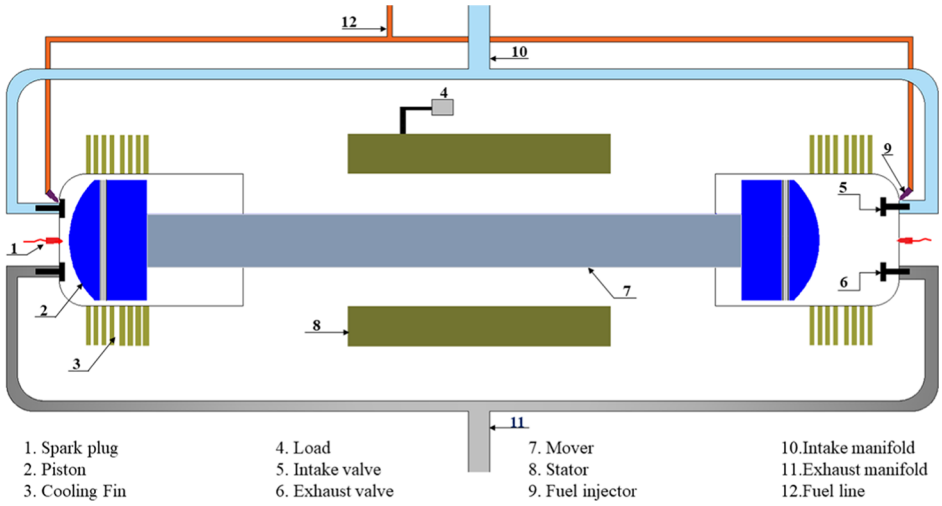

Figure 1. FPEG schematic configuration.

Toyota[15] has also developed a FPEG prototype system that operates in two-stroke mode with a single gas spring chamber, single combustion chamber, and a linear generator. In recent years,[16] an oil cooling passage was built to improve the cooling performance of the piston. A series of tests determined that the system could be operated for extended periods with an advanced control algorithm even with the odd abnormal combustion event.

The sensitivity of the piston motion profile and its influence on combustion stability and net power generated were fully characterized, highlighting a TDC position of 45 mm and a compression ratio of 6 without consuming any electric energy during compression. The researchers also reported[16] that frequency and phase could be controlled successfully. An advanced linear generator control algorithm was later proposed, which realized simple harmonic oscillations. To control the piston dead center position, speed control commands for the system were determined based on the positional errors measured at the extremes of each stroke. To support the experimental work, a one-dimensional simulation model was used to investigate alternative control methods, and the conclusions were further confirmed with test data from the FPEG prototype.[17]

West Virginia University[18] has developed a spark-ignited dual-piston engine generator. They reported the details of a spark-ignited system able to generate 316 W at 23.1 Hz. At low load, they reported high cycle-to-cycle variations (19.9%) in terms of the in-cylinder pressure histories and compression ratio and highlighted the impact of mixture preparation issues for both the fuel/air mixture and residual gases as the most likely source.

Sandia National Laboratory[19] has also developed a dual-piston FPEG. The system was designed[20] to operate using the homogeneous charge compression ignition (HCCI) mode and for a variety of fuels. This work demonstrated HCCI combustion with hydrogen at low equivalence ratios with compression ratios ranging from 20:1 to 70:1 with high corresponding indicated thermal efficiencies of 50−55%. Nevertheless, control proved challenging and test durations were short. A limited number of extended duration tests did demonstrate a path to indicated thermal efficiencies of >55%.

There have been other FPEG prototypes reported. For example Xu, et al. have demonstrated a single-cylinder four-stroke FPEG prototype using a linear generator and a mechanical spring for a rebound system.[21] Beijing Institute of Technology has developed a two-stroke, two-cylinder spark-ignited FPEG prototype, and successfully demonstrated cold start-up, combustion with gasoline and a generating process.[22−24] A compression ignition two-cylinder FPEG prototype was developed in parallel by the same team, and successful combustion was also reported.[25,26] A prototype dual-piston type spark ignition FPEG was built by Jaeheun Kim, et al.; liquefied petroleum gas (LPG) was used as the fuel.[27]

Zhang and Sun[28] stated that when seven renewable fuels like ethanol, biodiesel, hydrogen, etc., are considered for trajectory-based combustion control enabled by FPEG, it was found that FPEG has the highest flexibility of fuel compared to others. The work of Roman Virsik[29] compared FPEG with other range-extender technologies available and then has concluded that FPEGs with the use of internal combustion engines (ICEs) are feasible and has higher efficiencies with lower emissions and NVH values. This can be implemented in vehicles. Heron Rinderknecht[30] in their work compared several range-extender technologies for electric vehicles. They compared the FPEGs, polymer electrolyte fuel cells (PEFCs), turbine range extenders (TREs), and ICEs. Even though the fuel cells have higher efficiency than the FPEGs, they are not extensively used because of the inadequate infrastructure of hydrogen, its high cost, and the issues of storing hydrogen. When compared with TREs and ICEs, FPEGs have higher efficiency.

For a detailed review of free-piston engine technology, see Mikalsen et al.;[1] Raide et al.;[31] Wang et al.;[32] Woo and Lee;[33] and Hung and Lim.[34]

1.3. Aims and Methodology. As described, there have been a few prototypes reported on the FPEG concept; however, only a limited number of them have been realized and even fewer achieved successful combustion and electricity generation.

The article aims to go beyond the existing research and consider the reality of what a commercial FPEG system might look like in practice and estimate its size and weight based on a practical design development exercise. For context with other EV-range-extenders or hybrid technologies, it presents a promising design and compares it with relevant alternatives in terms of both size and weight.

The design employed and its operation is built upon a series of robust numerical modeling studies carried out over recent

https://dx.doi.org/10.1021/acs.energyfuels.0c01647
Energy Fuels XXXX, XXX, XXX−XXX

years[22−26] This work presents the realization of this concept in hardware in a proof-of-concept prototype form, thus representing a significant advancement of the FPEG concept itself.

This work is novel as it brings forward (a) a detailed technical packaging and sizing analysis of the merits of commercial FPEG prototype systems and compare it with other EV hybrid and range-extender technologies; (b) the details of a prototype experimental set-up, the data acquisition system, its control and actuation, and (c) to complete the work, it shows the initial experimental performance results obtained from the prototype.

The following sections set out the specifics of the concept in Section 2, together with its novelty, commercial design and compare its likely size and weight with its alternative technologies. In Section 3, the article presents the technical details and experimental set-up of the prototype system. In Section 4, the first data from the operation of the system are presented, summarized, and discussed.

2. HYBRID-VEHICLE FREE-PISTON ENGINE GENERATOR

2.1. Dual-Piston Concept Engine. The design of a dual-piston FPEG used for this work is based on the patent produced by Mikalsen and Roskilly.[35] A schematic of this system is presented in Figure 1. The FPEG concept is comprised of two opposing internal combustion free-piston engines and a linear electric machine. Each of the two free-piston engines has a combustion chamber comprised of a spark electrode (1), piston (2), and set of poppet valves (5 and 6). The linear electric machine (8) is located centrally between the cylinders/pistons. The electric machine can be operated as a motor or generator. The two pistons are connected using the mover (7) of the linear electric machine and this component as a whole represents the only significant moving part of the system.

In general terms, the starting process is initiated by operating the linear electric machine as a motor thus driving the system and piston motion and compressing and expanding the working fluid. However once established, the system is operated at steady state and the linear machine operates more as a generator. Combustion takes place alternatively in each cylinder, which drives the piston mover assembly in an oscillatory motion. The motion of the piston is linear only and using the linear electric generator is directly converted into electrical energy.

As there is no rotational motion, there is no need for a camshaft, which means that the valve actuation and timing must be controlled using an alternative linear-based system. Finally, the majority of reported dual-piston FPEG configuration uses a conventional two-stroke thermodynamic cycle; however, the same hardware employed in the current configuration can also be applied to also support a four-stroke thermodynamic cycle. This is achieved by simply timing valve open and close times accordingly and performing the intake and compression strokes separately from the expansion and exhaust strokes.

2.2. FPEG Design for an Electric-Vehicle Range-Extender or Hybrid Applications. An electric vehicle (EV) range-extender or hybrid electric application is shown in Figure 2 for a FPEG. It is expected that a FPEG will act as an on-board generator, charging an on-board electrochemical battery.

The rest of the system is similar to an EV, with the driver controlling the motor to turn the axles/wheels. When the charge in the electrochemical battery reaches a predefined state-of-charge, the FPEG will then be turned-on to generate more electricity.

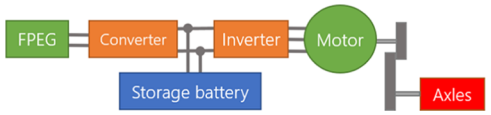

Figure 2. Example of FPEG implementation as a series hybrid technology with multiple FPEGs.

Fuel-to-electricity conversion efficiency is a clear and well-documented advantage for FPEGs, but it is only one aspect which is of importance to vehicle designers. In practice, the packaging and weight constraints of range extenders are also a major factor in range-extender or hybrid powertrain technology selection and vehicle powertrain design and layout. As such, to characterize the geometrical size and weight of a free-piston engine, a design study for a commercial design was carried out. The design exercise was completed using a combination of SolidWorks design tools and directly built upon the experience of establishing five free-piston engine/expander prototype designs and demonstration units across multiple projects. This included the prototype described in Section 3 and that of a recently designed linear Joule engine generator.[36]

Presented in Figure 3 is a three-dimensional (3D) cutaway image of a four-cylinder free-piston engine generator based upon

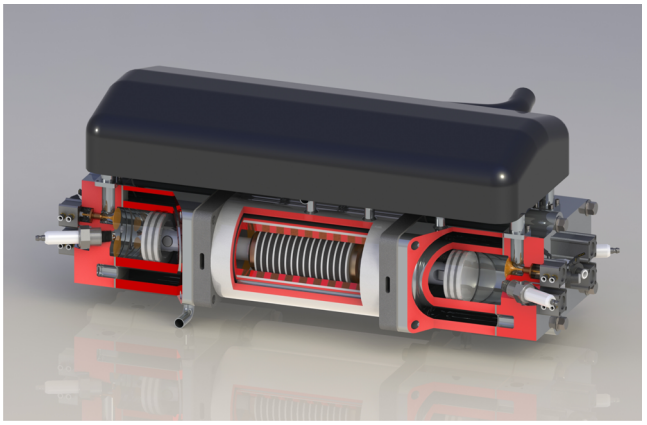

Figure 3. Design cutaway of a 24 kW_e FPEG for a EV-range-extender or hybrid powertrain. Image shows from left to right: a left combustion chamber (presented with piston, spark plug overhead valves), a left connecting rod, central linear machine, a right connecting rod, and the right combustion chamber (presented with piston, spark plug overhead valves).

the above concept. This unit has been designed to meet a 24 kW_e electrical output demand and has the design parameters shown in Table 1. The solution combines two dual-piston arrangements which are positioned in parallel (one arrangement is shown cutaway and the second behind), to minimize vibration and NVH (noise, vibration, and harshness); the motion of the pistons are timed to operate out of phase. Two linear machines are located in the center of the engine; these are driven by cylinders located at either end; the overhead valves are controlled pneumatically (or hydraulically) with a conventional spark plug system. The linear machine and cylinders are cooled using a water jacket design. In the figure, the intake and exhaust systems are located above and below the design correspondingly; however, the system could, in principle, be mounted or positioned vertically, horizontally, or upside down without issue.

As part of a hybrid-electric vehicle powertrain, the FPEG would be expected to operate largely at steady state and any

https://dx.doi.org/10.1021/acs.energyfuels.0c01647
Energy Fuels XXXX, XXX, XXX−XXX

Table 1. FPEG Prototype Specifications

parameters	value	unit
cylinder bore	60.0	mm
maximum stroke	60.0	mm
moving mass	1.5	kg
max. intake/exhaust valve lift	5.0	mm
intake valve diameter	15.0	mm
exhaust valve diameter	15.0	mm
electrical power output	24.0	kW_e
gravimetric power density	0.53	kW_e/kg
volumetric power density	2.43	kW_e/L
total mass	44.3	kg
total volume	9.85	L

transient loading imposed by the driver/journey would be met through on-board battery or capacitor storage.

The design process yielded a design which on a component basis broke down according to that shown in Figure 4.

As shown, the system has been presented in terms of the mass/volume of the electric linear machine and its housing, the cylinder head and its system components (spark plug, injectors, and overhead valves), and the cylinders themselves. In general, a third of the total mass/volume of the system comes from the linear machine section.

As different power conversion devices often come with different power specifications, for simplicity, we present the data in terms of their specific power density, i.e., if we define the gravimetric power density, g as

$$g = \frac{P_e}{m} \tag{1}$$

where m is total system mass and P_e is the total electrical power output. We can then define the volumetric power density, v as

$$v = \frac{P_e}{V} \tag{2}$$

where V is the total system volume.

In the FPEG system, compared to conventional reciprocating internal combustion engine range-extender/hybrid power systems, the need for a crankcase has been removed, thus yielding an improved gravimetric and volumetric power density.

Presented in Figure 5 is a comparison with other well-known hybrid/range-extender technologies found across the technical literature at different stages of research, prototype, and commercial development. These include small-scale reciprocating engine gasoline-fueled genset,[37,38] conventional state-of-the-art gasoline-fueled reciprocating engine for automotive applications,[39,40] conventional gasoline-fueled range extenders,[41−43] rotary engines,[4445] and fuel cells.[46]

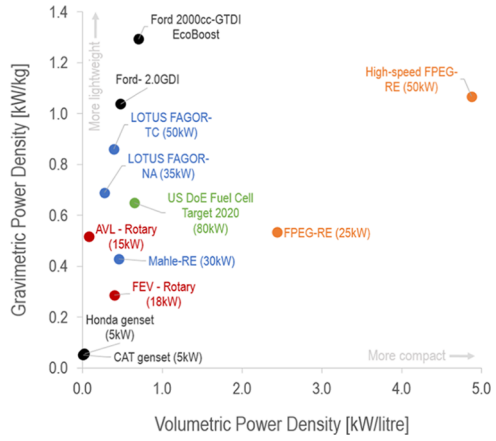

Figure 5. Alternative on-board electrical and mechanical generators in terms of gravimetric and volumetric power density of the whole power unit. Labels: CAT genset (5 kW_e)[37]—microgenerator set powered by gasoline; Honda genset (5 kW_e)[38]—microgenerator set powered by gasoline; Ford 2.0 L—GTDI EcoBoost[39]—a state-of-the-art diesel engine (not including the additional electrical generator); Ford 2.0 L—GDI[40]—a state-of-the-art gasoline engine (not including the additional electrical generator); Lotus FAGOR-TC (50 kW_e)[41,42]—A turbocharged gasoline internal combustion engine range extender; Lotus FAGOR-NA (35 kW_e)[41,42]—naturally aspirated gasoline internal combustion engine range extender; AVL-rotary (15 kW_e)[44]—concept rotary engine range extender; FEV-rotary (18 kW_e)[45]—concept rotary engine range extender; Mahle-RE (30 kW_e)[43]—internal combustion engine range extender; Fuel Cell Target 2020 (80 kW_e);[46] FPEG-RE (25 kW_e)—a four-cylinder 25 Hz variant of the FPEG presented in ref 47; high-speed FPEG-RE (50 kW_e)—a four-cylinder 50 Hz variant of the FPEG.[47]

As presented, the proposed 24 kW_e FPEG has great potential to offer a competitive solution to the alternatives in terms of

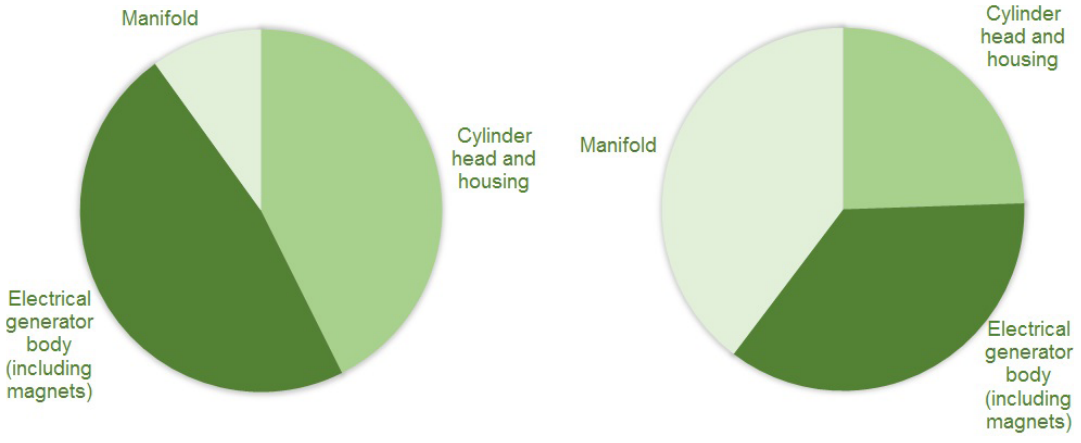

(a) Breakdown in gravimetric terms (b) Breakdown in volumetric terms

Figure 4. Percentage breakdown of the sections of a commercial FPEG design.

https://dx.doi.org/10.1021/acs.energyfuels.0c01647
Energy Fuels XXXX, XXX, XXX−XXX

gravimetric power density. However, there is a notable improvement compared to the alternatives in terms of volumetric power density with the FPEG offering a design that is around twice as compact than the best alternative. The design specification offered in Table 1 is based around a 25 Hz operational speed; this corresponds to the equivalent of 1500 rpm, most spark-ignited internal combustion comfortably operate at 3000 rpm; hence, a FPEG operating at 50 Hz could potentially be technically feasible. The power density of such a FPEG is also presented in Figure 5. The analysis shows that such a design would offer the same scales of gravimetric power density offered by conventional automotive reciprocating engines but with an integrated electrical generator but up to 80% smaller.

3. RESEARCH PROTOTYPE FREE-PISTON ENGINE

In an effort to demonstrate the concept outlined in Section 2.1, an experimental system has been designed and manufactured. A comprehensive description of this system can be found in ref 48. As one might expect, the free-piston engine prototype comprises all of the systems essential to the operation of an internal combustion engine. In general, these have all been procured as subcomponents and used to assemble the whole system, for example, the two-cylinder units were originally from a commercial Stihl 4-MIX spark ignition engine. This modification meant that the crankshaft and flywheel of the Stihl 4-MIX were removed, and a cylinder base was added to close the lower section of the cylinder. A Festo pneumatic system has been developed to activate to open and activate to close the overhead intake and exhaust valves. Nominally, the valve lift is designed to be 4.0 mm; however, the design supports this to be adjustable, which allows for greater control as well as enables further optimization of the valve operation. The main pneumatic air supply is provided at 6.0 bar via a manifold before being connected via a 6.0 mm tube to the main pneumatic actuation cylinder. This valve actuation system has been tested independently, with a less than 8.0 ms opening latency (signal to maximum opening) and a 20.0 ms latency on closing. In practice, this enables for the overall FPEG system to be operated comfortably with operational speeds in the range of 10.0−15.0 Hz.

An electronic port fuel injection (EPI) system is employed, as in reciprocating internal combustion engines, the assembly consists of an intake manifold with an injector, throttle, and fuel pump. In the current work, gasoline was selected as the input fuel; in the following work, standard gasoline fuel (Unleaded petrol BS EN 228:2012) was adopted. The injection timing and injection frequency are set using a CompactRIO system by National Instruments with a bespoke injection control algorithm developed in LabVIEW by the team. The ignition system used in this prototype is identical to those used reciprocating internal combustion engines. It is comprised of an oscillator-transformer-rectifier circuit, a 12 V battery, a capacitor, and coil. The 12 V battery is stepped up to higher voltage (20 kV) by the ignition system. To enable real-time measurement of in-cylinder pressure, a Bosch spark plug has been selected for this prototype, which has an integrated pressure sensor produced by AVL (Model ZI21).

The piston rings were retained from the commercial Stihl 4-MIX base engine; these were lubricated using conventional lubrication oil, which was dripped onto the piston side at the bottom dead center (BDC).

3.1. Linear Electric Machine. The linear electric machine used in the FPEG prototype has multiple functions which are:

1. To operate as a motor during start-up and to drive the piston up to the required compression ratio for ignition;
2. To operate as a generator to produce electricity during stable operation with the electrical current generated from the alternator coil; and
3. To operate as a motor for the four-stroke engine during start-up and during the nonpower stroke.

Nevertheless, the current availability for commercial linear motors in the 10 s kW_e size is limited, with most designed for smaller-scale process engineering and manufacturing applications rather than specifically for electricity generation. After an extensive process,[48] a linear motor (Moog Model 50204D) was adopted due its high power density and ability to provide sufficient force during the starting process.

The motor drive used was the Parker model Compax3H, the system needed to be configured using C3 Manager Software via a RS232 connection to a master control computer. Initially, the motor was driven using a sinusoidal electrical commutation of three-phase coils. The mover position, velocity, and acceleration information are provided by the linear encoder and are used as feedback to the mover master control system. The control parameters that are required to be manually entered in the motion control software include mover starting and stopping positions, speed, acceleration, etc., which set the motion profile.

3.2. Data Acquisition. The data acquisition and control are implemented in parallel using the National Instrument CompactRIO system, under the management of a program written and uploaded to the system via the LabVIEW software. All sensors and actuators are connected to I/O modules on the CompactRIO system, and the data collected is stored in the CompactRIO memory temporarily and then streamed and visualized in real time on a host PC. This data is then postprocessed using a MATLAB script.

3.3. FPEG Prototype. The FPEG prototype developed is illustrated in Figure 6. In the current study, the two-stroke operation under spark ignition combustion mode is adopted. The poppet valves are used for both intake and exhaust processes rather than scavenging ports. By applying intake and exhaust valves with independent timing control, the gas exchange process can then decoupled from the piston motion. The prototype specifications are listed in Table 2.

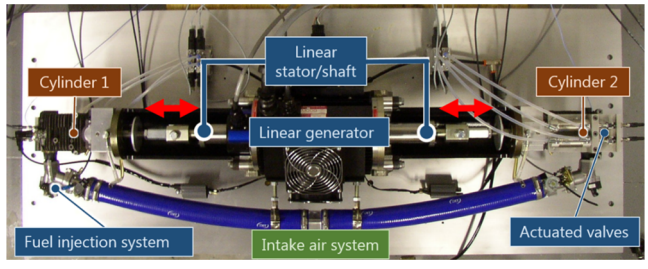

Figure 6. FPEG prototype at Durham University.

4. EXPERIMENTAL RESULTS

4.1. System Motoring. The linear electric machine is operated as a motor during the current stage, to drive the piston assembly to reach the required conditions for ignition. After combustion, the linear electric machine works as an active controller to control the piston to move according to a preset displacement profile. The target piston displacement is shown in Figure 7; throughout this study, this is a sinusoidal wave function. The piston dead center is 17.0 and −17.0 mm from the middle position of the stroke, and clearance from the cylinder

https://dx.doi.org/10.1021/acs.energyfuels.0c01647
Energy Fuels XXXX, XXX, XXX−XXX

Table 2. FPEG Prototype Specifications

parameters	value	unit
cylinder bore	50.0	mm
maximum stroke	40.0	mm
moving mass	7.0	kg
max. intake/exhaust valve lift	4.0	mm
intake valve diameter	20.0	mm
exhaust valve diameter	18.0	mm

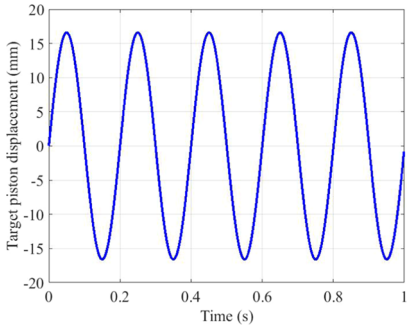

Figure 7. Target piston displacement with an active controller.

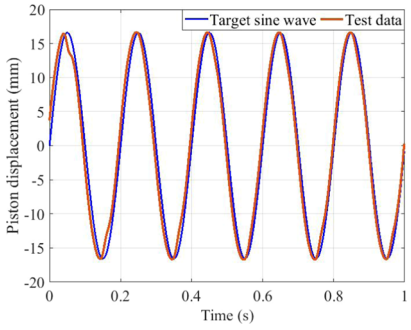

Figure 8. Comparison of tested displacement with target displacement.

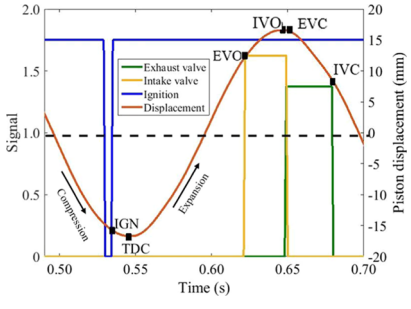

Figure 9. Control signals for the left cylinder.

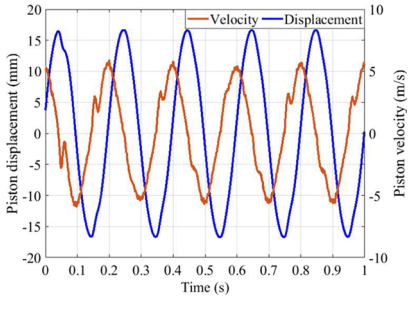

Figure 10. Piston dynamics.

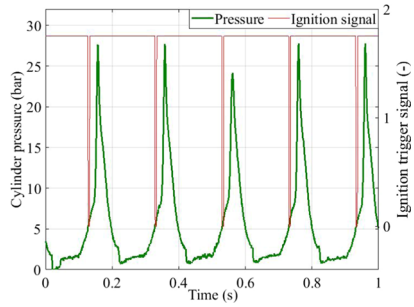

Figure 11. Cylinder pressure in the left cylinder.

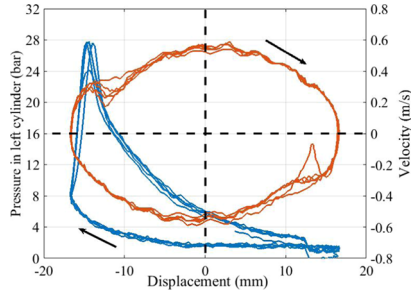

Figure 12. Cylinder pressure in the left cylinder with displacement (orange—velocity, blue—pressure in the left cylinder).

Table 3. FPEG Prototype Base Case

parameters	value	unit
operational speed	5.0	Hz
stroke	34.0	mm
compression ratio	3.7	
air/fuel equivalence ratio	1.0	
reference position (ref)	15	mm
top dead center (TDC)	0.059	s aRef
bottom dead center (BDC)	0.16	s aRef
spark timing	−0.014	s aTDC
inlet valve open (IVO)	−0.034	s aTDC
inlet valve close (IVC)	0.006	s aTDC
exhaust valve open (EVO)	0.039	s aBDC
exhaust valve close (EVC)	0.077	s aBDC

head is 4.0 mm. This corresponds to a compression ratio of 3.7. In the presented test, the piston oscillates between its two dead centers, and the time duration for one operating cycle is 0.2 s, with a corresponding frequency of 5 Hz. The current operating speed of the designed FPEG prototype is the equivalent of 300 RPM, which is much lower than a conventional reciprocating engine (800−4000 RPM). In both the selection of engine speed and compression ratio, conservative values have been adopted to support improved control and minimize the risk of piston head/cylinder head impact. The adopted speed enables the engine ignition system, valve system, and injection system to have sufficient time to respond. On-going testing is looking at how this can be further improved by changing the frequency of the target piston displacement of the controller (to date successfully operated at 11 Hz) and by optimizing the operating conditions of the prototype to make sure the piston follows the target profile without undesirable delay.

The tested piston displacement is compared with the target profile, to validate the feasibly of the control strategy and test response time of the prototype. The comparison results are shown in Figure 8. If an extremely high frequency is adopted to the prototype, the engine subsystem may well fail to respond in time. It seems that the piston motion becomes stable after the first few operating cycles, then follows the target profile. As time progresses, as the number of cycles increases, the piston-position control parameters calibrate to better meet the

https://dx.doi.org/10.1021/acs.energyfuels.0c01647
Energy Fuels XXXX, XXX, XXX−XXX

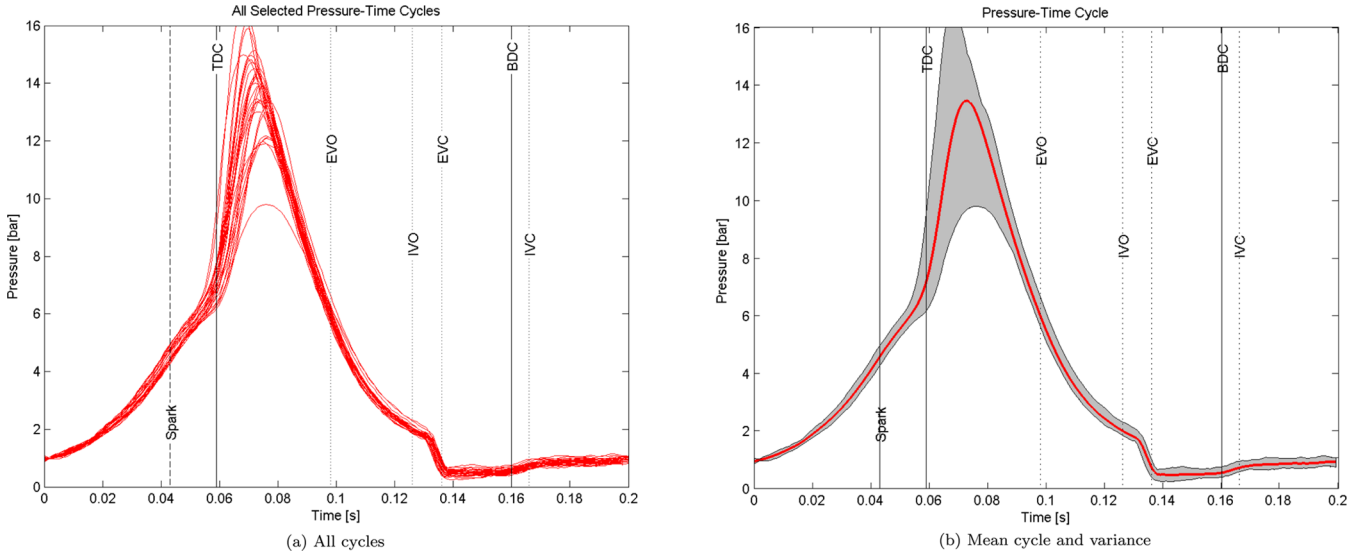

(a) All cycles (b) Mean cycle and variance

Figure 13. In-cylinder pressures vs time with stoichiometric air/fuel ratio at 5 Hz (left-hand side cylinder).

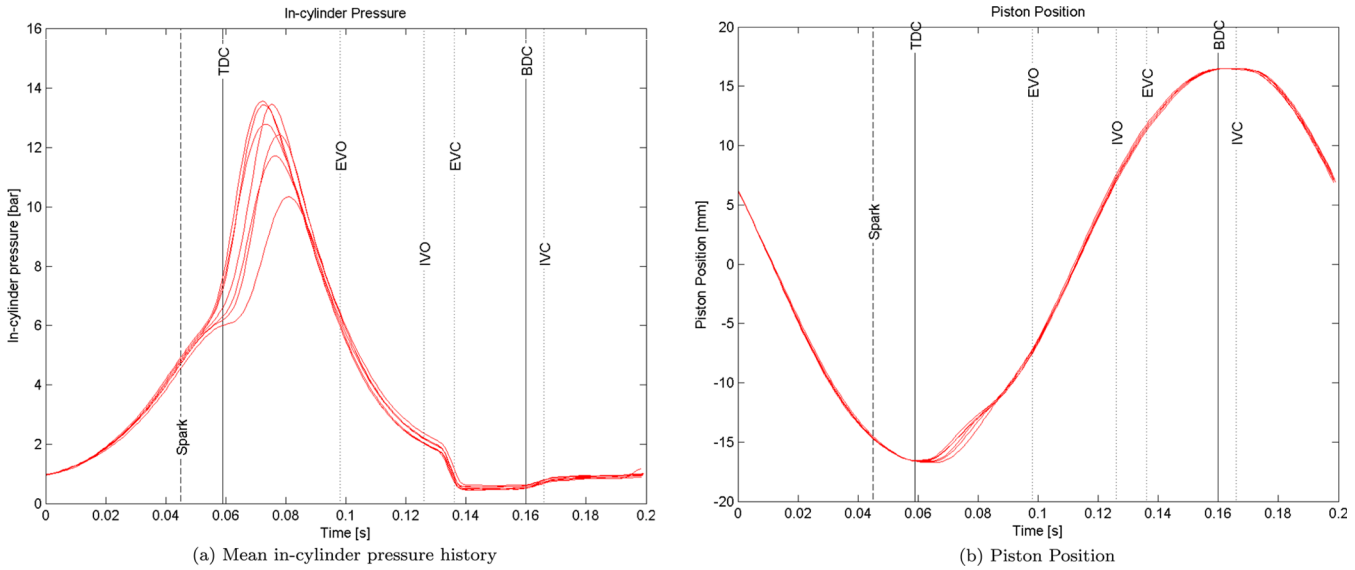

(a) Mean in-cylinder pressure history (b) Piston Position

Figure 14. Spark ignition timing sweep (left-hand side cylinder).

target displacement profile. Thus, the real-time piston displacement is controlled to move in a sinusoidal wave despite the initial disturbance to the FPEG system.

The current FPEG prototype is operated based on a two-stroke thermodynamic cycle; intake air is supplied through an airline to facilitate gas exchange and also to boost the intake manifold pressure (boosted to an absolute pressure of 1.2 bar). The spark ignition event and valve timings are initiated based on piston displacement and velocity as feedback. The control signals for the ignition event and valve for the left cylinder are illustrated in Figure 9. The spark ignition is triggered at the end of the compression stroke before the piston reaches its TDC (top dead center). The scavenging process for the two-stroke operation cycle is a combined intake and exhaust gas exchange process, i.e., exhaust valve opening (EVO) is actuated before intake valve opening (IVO) and exhaust valve closing (EVC) is actuated after intake valve closing (IVC). The current valve timings were not optimized at this stage.

4.2. Power Generation. The FPEG was then operated at 5 Hz with fuel supplied and an ignition event triggered, resulting in a combustion event. Presented in Figure 10 are the corresponding results of the test in terms of piston displacement and its velocity. As shown in the figure, five separate compression and expansion events are observed. The profile typically achieves a ±17mm displacement; however, compared to the control displacement target (a sine wave), shown in Figure 7, the profile target across the whole cycle is not always achieved. As velocity is the derivative of displacement, the impact of pressure rise due to combustion and thus piston position is more apparent in the figure.

The in-cylinder pressure and ignition signal for the spark over a second or five cycles are presented in Figure 11 for the left-side cylinder. Initiated by the ignition signal and spark, the observed combustion and pressure profiles appear very similar to those reported in reciprocating internal combustion engines. As might be expected, the peak pressure timings corresponded to the perturbations observed in the piston displacement velocity presented in Figure 10.

The outcome in terms of pressure vs displacement is presented in Figure 12. As shown, work is done by the expanding gas on the piston and the piston velocity typically follows an "oval-like" profile moving in the clockwise direction. Any perturbations are driven by the combustion event and growing pressure either in phase with events in the left or right cylinder. However, once the cycle has progressed to −8.0 or 8.0 mm, the perturbations have been smoothed and the piston follows a similar profile.

The pressure vs displacement plot shows similar behavior, showing only minor differences in the displacement domains.

https://dx.doi.org/10.1021/acs.energyfuels.0c01647
Energy Fuels XXXX, XXX, XXX−XXX

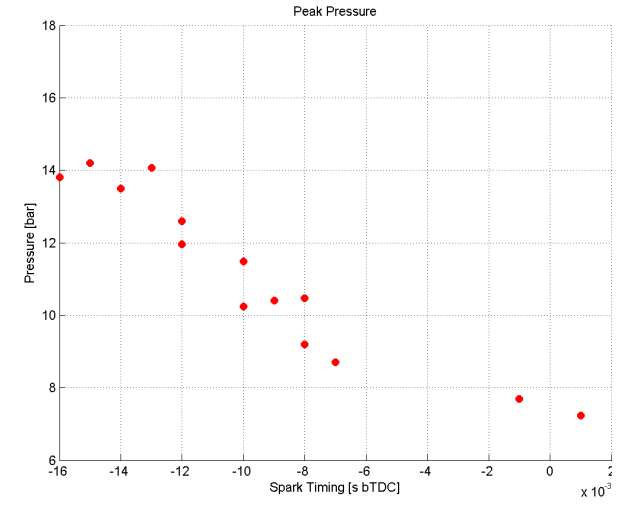

(a) Peak Pressure

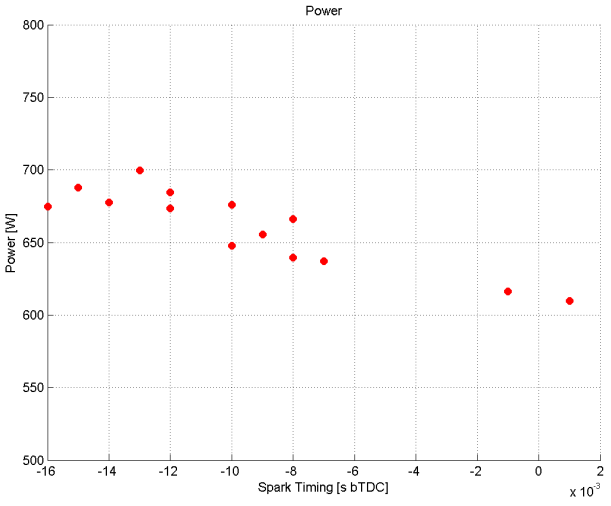

(c) Indicated Power

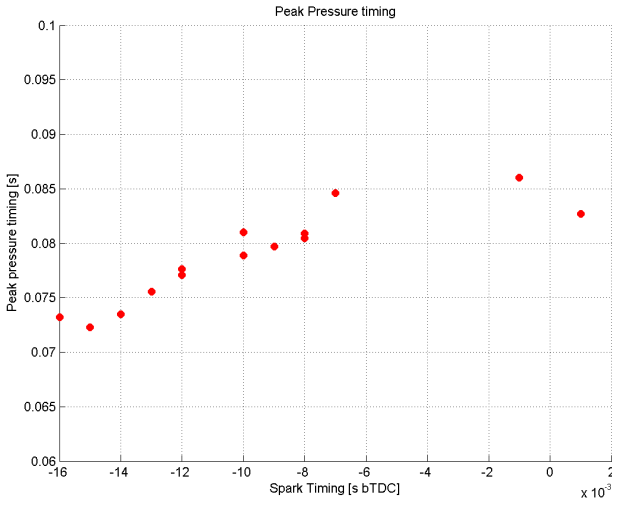

(b) Peak Pressure Timing

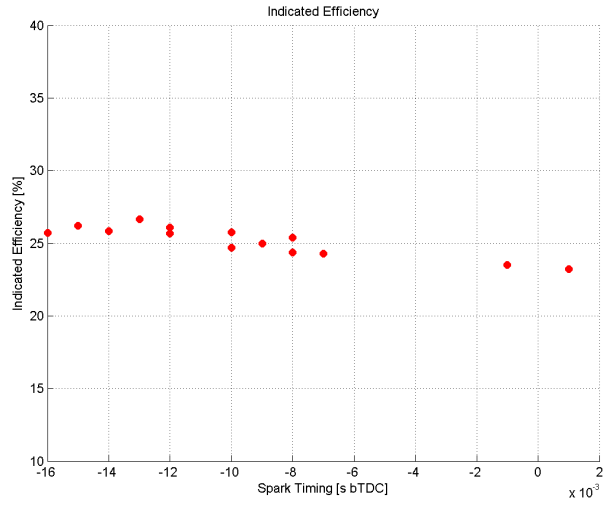

(d) Indicated Efficiency

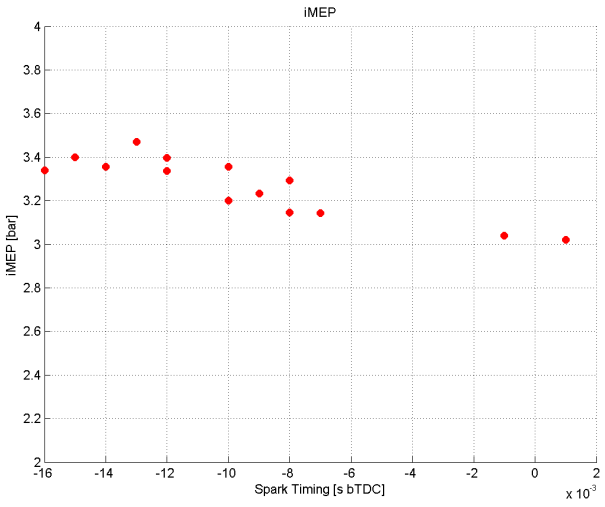

(e) Indicated Mean Effective Pressure

Figure 15. Spark ignition timing sweep—mean parameters (left-hand side cylinder).

4.3. Base Operational Case. During a series of engine tests, the in-cylinder pressure data was collected over 30−50 consecutive combustion cycles; these data were postprocessed and analyzed in further detail. After a significant test program that sort to optimize the operation of the FPEG prototype in terms of intake open/close valve timing, exhaust open/close valve timing, and spark ignition timing, a base case was identified at 5 Hz and with a stoichiometric air/fuel ratio, summarized in Table 3. The trends observed in the left cylinder were

https://dx.doi.org/10.1021/acs.energyfuels.0c01647
Energy Fuels XXXX, XXX, XXX−XXX

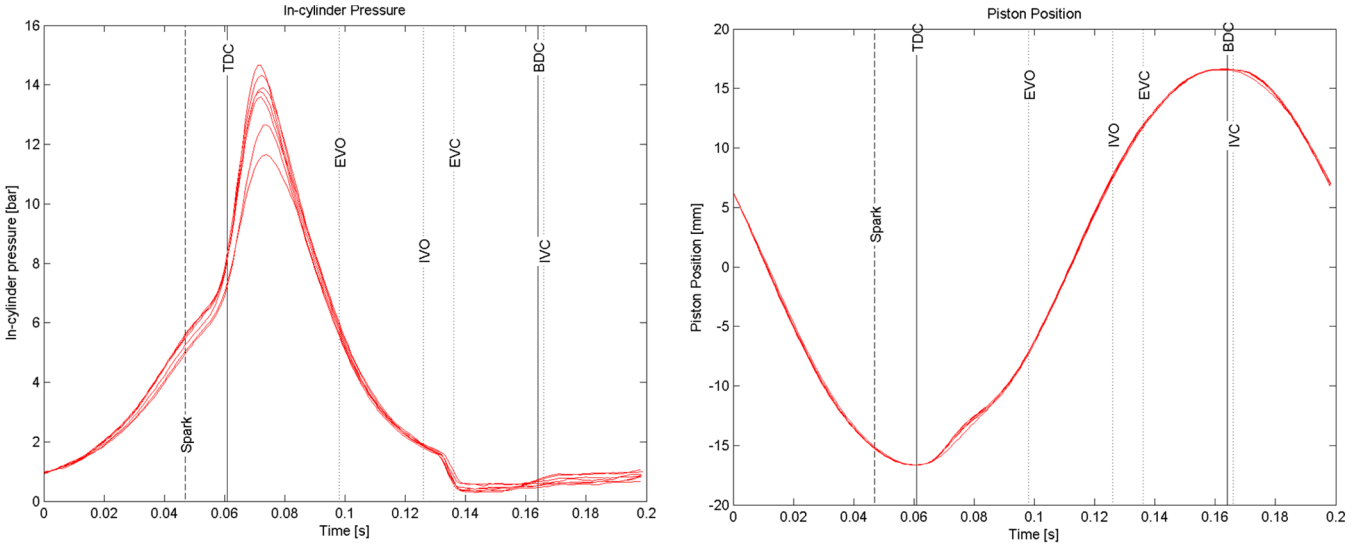

(a) Mean in-cylinder pressure (left side)

(b) Piston Position

Figure 16. Intake timing sweep (left-hand side cylinder).

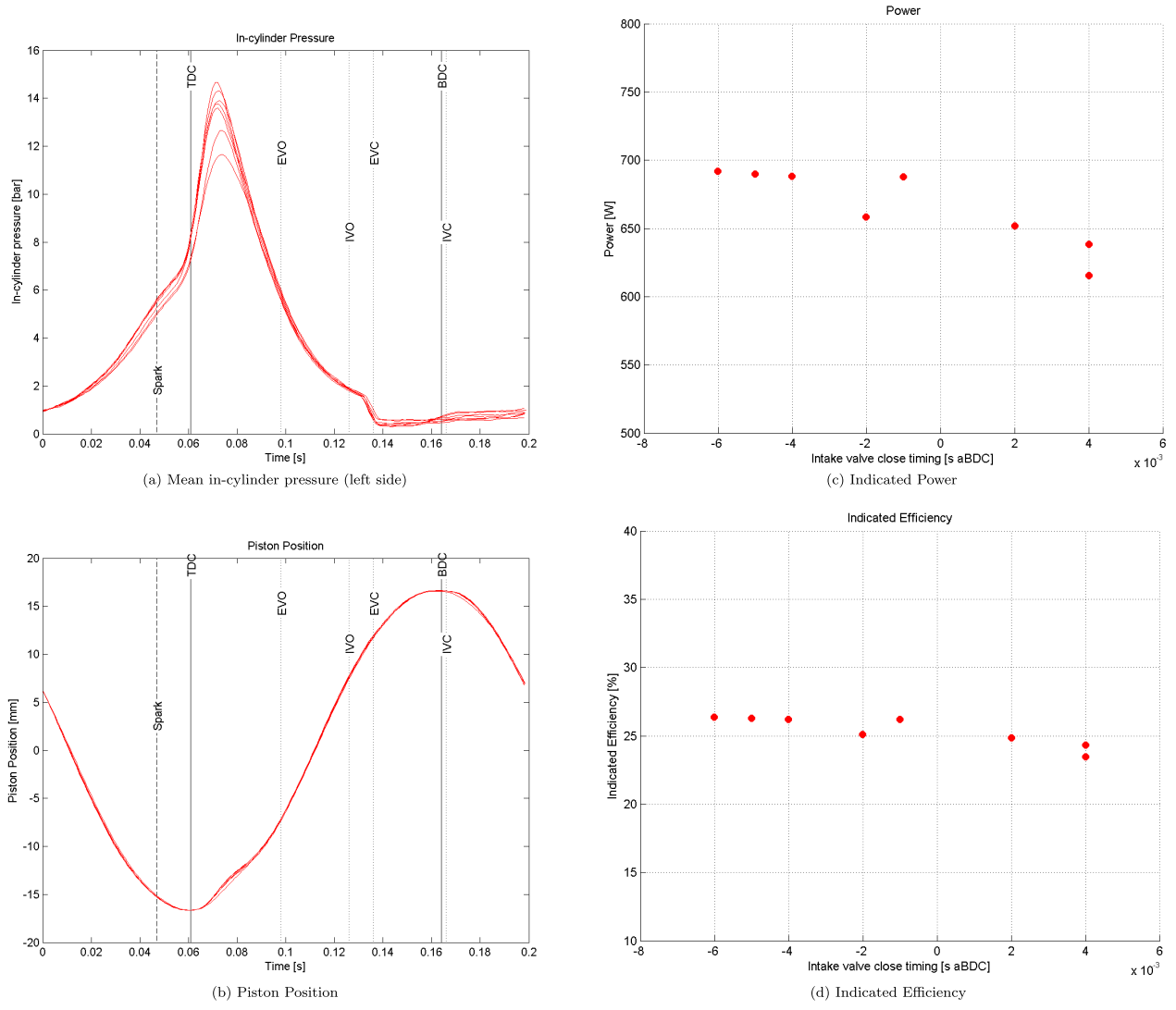

(a) Mean in-cylinder pressure (left side)

(c) Indicated Power

(b) Piston Position

(d) Indicated Efficiency

Figure 17. Intake timing sweep—mean parameters (left-hand side cylinder).

https://dx.doi.org/10.1021/acs.energyfuels.0c01647
Energy Fuels XXXX, XXX, XXX−XXX

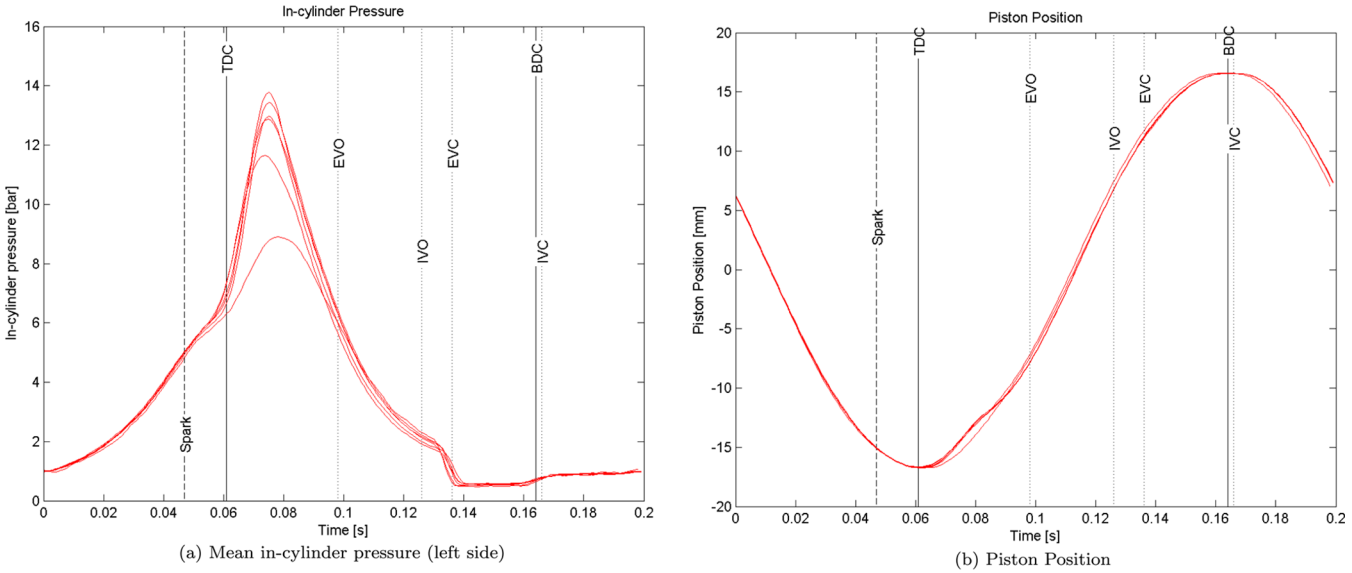

(a) Mean in-cylinder pressure (left side)

(b) Piston Position

Figure 18. Exhaust timing sweep (left-hand side cylinder).

generally mirrored in the right cylinder, thus from hereon only the data obtained in the left cylinder are discussed.

An example of the resulting cycles for this cycle is shown in Figure 13. With a consistent spark timing, in-cylinder cycle-to-cycle variation is observed. This observation is consistent with conventional spark ignition engines (with the source of these variations a function of the quality of mixture preparation, i.e., fuel evaporation, valve timing closure/opening timing precision, in-cylinder turbulence/flame interaction, etc.). As such throughout this work, a mean cycle is presented and discussed (shown in red). On-going work[49] using the same prototype but with hydrogen gas fueling indicated that the most significant contribution to cyclic variation and the explanation of the observed variance currently relates mainly to the quality of the gasoline−air mixture preparation rather than any fundamental control issue.

4.4. Parametric Sweeps. To characterize the impact of ignition timing, intake valve closing time, and exhaust valve closing time, a series of parametric sweeps were undertaken which related these control parameters to operational characteristics such as peak pressure, peak pressure timing, indicated power, indicated efficiency, and indicated mean effective pressure (iMEP).

The peak pressure was defined as the maximum pressure observed during a combustion cycle; the peak pressure timing was the time in milliseconds after top dead center (aTDC), where that peak pressure was recorded.

The indicated power, indicated efficiency, and indicated mean effective pressure (iMEP) were all derived from standard reciprocating internal combustion engine parameters.[50]

The real engine cycle of an internal combustion engine can be illustrated by mapping the pressure−volume (PV) data extracted from a pressure versus volume diagram. An example of this (albeit in terms of piston displacement rather than volume) is presented in blue in Figure 12.

The area under the curve is the indicated work per cycle, W as given by the following equation, where p is the cylinder pressure and V is the cylinder volume.

$$W = \int p\mathrm{d}V \tag{3}$$

The indicated power can be derived from the indicated work per cycle, W by multiplying by the frequency, f. The indicated mean effective pressure (iMEP) is the time-averaged in-cylinder pressure.

The indicated efficiency is the percentage of indicated power produced relative to the supplied chemical energy in the fuel.

4.4.1. Spark Ignition Timing. The spark ignition timing was varied from −16.0 to 2.0 ms aTDC (after top dead center); the results are shown in Figures 14 and 15. The limits were not due to system hard limits; these were set by the operators who identified that operational pressures were possibly too high (when most advanced) for comfortable operation or might limit exhaust valve opening performance (when most delayed).

In all cases, the mean value or cycle is presented. Unfortunately, due to some noisy data with a spark timing at around −4.0 ms aTDC; this data was not able to be processed in full.

Across the data collected, it is apparent that a spark ignition timing sweep has much the same impact on the dynamic performance of a FPEG as would be expected in a conventional reciprocating spark ignition engine system, i.e., as spark timing is advanced, the timing and magnitude of peak pressure is also advanced and increased, respectively.

When focusing more specifically on the shape of the mean in-cylinder pressure profiles presented, it is clear that cycle-to-cycle variation described in Section 4 is affecting the analysis. For context, recently published data on hydrogen fueling[49] (unaffected by any liquid fuel mixture preparation issues) indicates that each of these profiles should not overlap after spark and during combustion. However, those shown in Figure 14 are overlapping particularly close to peak pressure. Thus, the observed trends rather than specific test points are the emphasis of the following sections.

Further analysis of these data indicated that the indicated power, indicated efficiency, and iMEP (indicated mean effective pressure) generally increased as the spark timing was advanced, maximizing at around −13.0 ms aTDC. This corresponded to 0.7 kW_e at 26% indicated efficiency.

Throughout the experiment, the exhaust opening time was fixed, thus later ignition times had less time before the valve was opened, resulting in lower efficiencies.

In general, the trends observed across the engine performance parameters appeared to follow a linear trend and showed the potential for optimizing performance through manipulation of the timing of combustion. Interestingly, no knocking combustion events were observed in any of the recorded cycles across this data set, even with more advanced spark timings.

4.4.2. Intake Valve Closure Timing. The duration of opening was fixed to 0.04 s and the intake valve closing (IVC) timing was set from −0.006 to 0.004 s aBDC (after bottom dead center). Outside this operating window, despite attempts to improve observed performance characteristics, it proved not possible to maintain stable in-cylinder combustion and experiments were halted.

https://dx.doi.org/10.1021/acs.energyfuels.0c01647
Energy Fuels XXXX, XXX, XXX−XXX

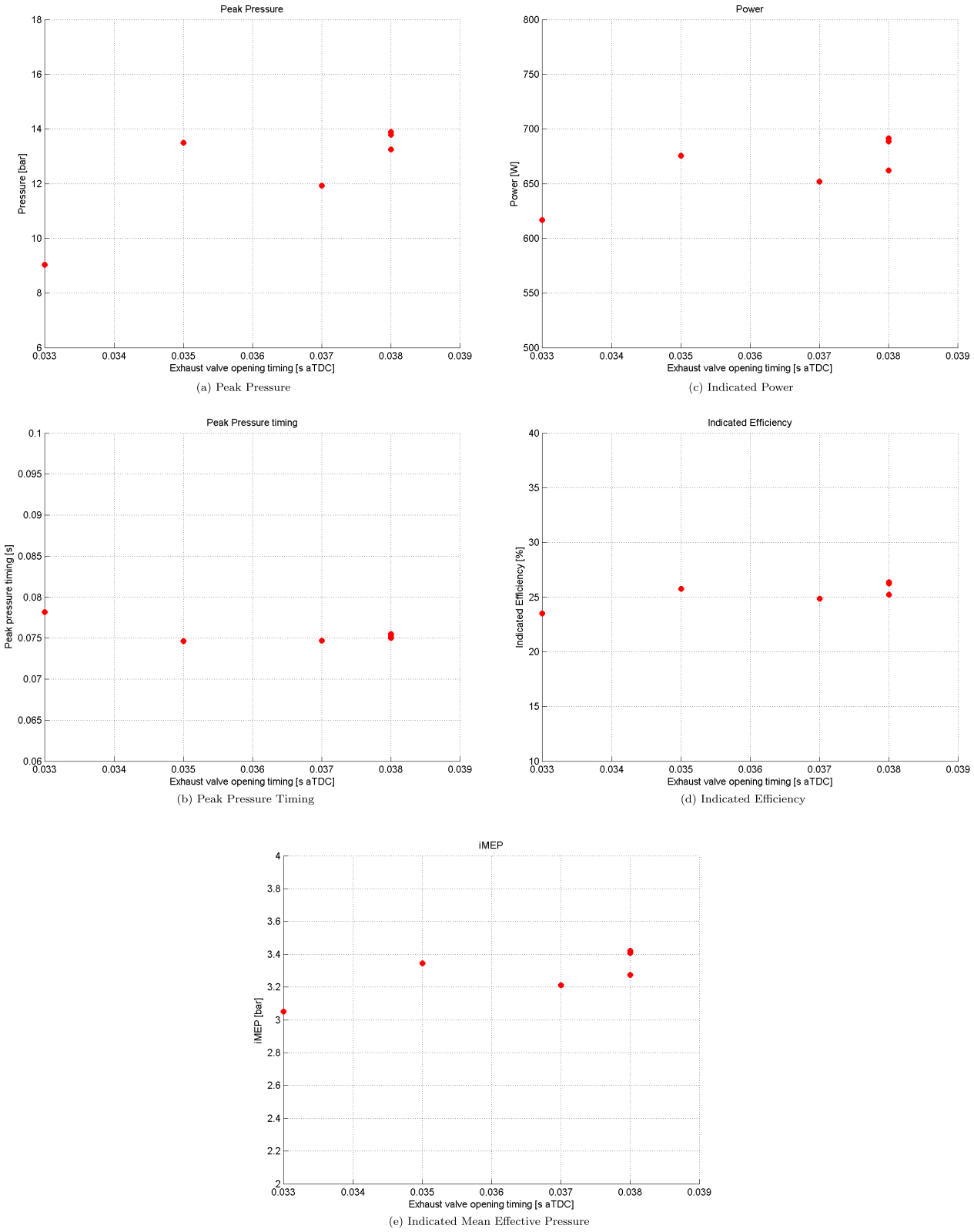

(a) Peak Pressure

(c) Indicated Power

(b) Peak Pressure Timing

(d) Indicated Efficiency

(e) Indicated Mean Effective Pressure

Figure 19. Exhaust timing sweep—mean parameters (left-hand side cylinder).

Presented in Figures 16 and 17 are the results of this intake valve timing sweep.

As IVC is delayed, the in-cylinder pressure is reduced as the less combustible mixture is trapped within the chamber. As a result, this yields lower pressures generally at spark ignition and thus resulting in a lower peak pressure. As such, as IVC is delayed, the peak pressure is reduced while its timing remains relatively steady across the whole sweep.

The reduced trapped combustible mixture yields lower indicated power, efficiency, and iMEP. Across the data set, earlier intake valve timings yielded the highest efficiencies and powers. This is likely to be associated with moving toward a more optimal point.

https://dx.doi.org/10.1021/acs.energyfuels.0c01647
Energy Fuels XXXX, XXX, XXX−XXX

While carry out the parametric sweep, the limits of the system were identified and between these points, the results again showed linear behavior with no significant differences between what might be expected in a two-stroke reciprocating engine. Hence, it is shown that the timing of the valve closing event could be considered as a potential option for engine performance parameter optimization.

4.4.3. Exhaust Valve Opening Timing. Finally, a sweep of exhaust valve opening (EVO) times was carried out using the prototype. In this case, the open duration was fixed to 0.038 s and a valve time sweep starting with an EVO of 0.033−0.038 s was completed in sequence. The results are presented in Figures 18 and 19. Much like the intake valve timing sweep, outside this operating window combustion was irregular and could not be sustained. Various attempts to maintain combustion with similar parameters were attempted with no success in extending these limits.

Delaying the EVO control parameter generally resulted in higher in-cylinder pressures but not to the timing of peak pressures, etc. However, compared to the other two parametric sweeps, the changes to EVO time yielded only minor differences to the observed performance parameters.

Much like the operation of a two-stroke reciprocating engine, it was considered that beyond the 0.033 and 0.038 s limits, the prototype was unable to scavenge the burned gases effectively. This resulted in noncombustible mixtures being created and thus no and irregular combustion events.

Nevertheless, while the performance of the prototype showed less sensitivity to the EVO control parameter in terms of power, efficiency, etc., compared to the intake and spark timing sweeps, it proved highly sensitive to the scavenging process.

5. DISCUSSION

The analysis of the volumetric and gravimetric densities shows that the potential system size and weight are likely to offer significant advantages over other hybrid EV powertrains. In the context of an EV, the internal packaging is a challenge with battery size likely to be maximized. Thus, any solution which better delivers on size and weight constraints has great potential.

The analysis shows that an indicated efficiency of around 26% was obtained at 5 Hz. For context, this practical efficiency should be considered as relatively high since the adopted compression ratio was only 3.7 and the system was operated at relatively low speeds and would have been very susceptible to high heat transfer losses. There remains much scope for increasing the speed to above 10−20 Hz and the compression ratio to 9.0 and beyond.

For example, for the purposes of a simple illustration, the ideal efficiency from gasoline-fueled internal combustion engines is generally based on the analysis of an Otto cycle[50]

$$\eta_{\text{ideal}} = 1 - \frac{1}{r_c^{\gamma-1}} \tag{4}$$

where r_c is the compression ratio (maximum in-cylinder volume to minimum in-cylinder volume ratio) and γ is the ratio of specific heats.

Therefore, with the compression ratio employed here, $r_c = 3.7$, and $\gamma = 1.35$ assuming the ideal efficiency, $\eta_{\text{ideal,CR=3.7}}$ can be approximated as 37%. In practice, this was realized at 26%. Hence, if the compression ratio, r_c, was increased to a more conventional 9.0, this would yield $\eta_{\text{ideal,CR=9}} = 54\%$. Thus, as would be expected, an increase in the system compression ratio would be expected to significantly improve the indicated efficiency. The next steps of the testing are currently focusing on increasing compression ratio and operating speed to maximize efficiency and power density.

6. CONCLUSIONS

The potential of a free-piston engine generator for electrical-vehicle range-extenders or hybrid powertrain applications is presented including the first results from a proof-of-concept prototype system. The outcomes can be summarized as:

1. A full-scale range-extender or hybrid design indicates that a FPEG offers excellent gravimetric and volumetric power densities compared to alternative range-extender and hybrid powertrain technologies.
2. A proof-of-concept FPEG prototype has demonstrated that combustion events can be controlled using the electric machine and is sufficiently repeatable.
3. The FPEG prototype has been operated successfully in two-stroke combustion mode with gasoline fueling.
4. Parametric sweeps of spark ignition, intake, and exhaust timings have supported the optimization of the system control, resulting in 0.7 kW_e per cylinder at 26% indicated efficiency.
5. Increasing the compression ratio from 3.7 to a more conventional 9.0 and increasing operating frequency would be expected to improve the efficiency in line with the expected high efficiencies.

AUTHOR INFORMATION

Corresponding Author

Andrew Smallbone − *Department of Engineering, Durham University,, Durham DH1 3LE, U.K.;* orcid.org/0000-0001-7843-8967; Email: andrew.smallbone@durham.ac.uk; www.durham.ac.uk/dei

Authors

Mohd Razali Hanipah − *Department of Engineering, Durham University,, Durham DH1 3LE, U.K.; Faculty of Mechanical Engineering, Universiti Malaysia Pahang, Pekan 26600, Pahang, Malaysia*

Boru Jia − *Department of Engineering, Durham University,, Durham DH1 3LE, U.K.; School of Mechanical Engineering, Beijing Institute of Technology, Beijing 100081, China*

Tim Scott − *SR Technology Innovations, Unit 2F, Littleburn Business Centre, Durham DH7 8ET, U.K.*

Jonathan Heslop − *Department of Engineering, Durham University,, Durham DH1 3LE, U.K.*

Ben Towell − *BNC Engineering Solutions Ltd, Front Offices, St James' United Reformed Church, Newcastle-Upon-Tyne NE1 8JF, U.K.*

Christopher Lawrence − *Department of Engineering, Durham University,, Durham DH1 3LE, U.K.; BNC Engineering Solutions Ltd, Front Offices, St James' United Reformed Church, Newcastle-Upon-Tyne NE1 8JF, U.K.*

Sumit Roy − *Department of Engineering, Durham University,, Durham DH1 3LE, U.K.*

K. V. Shivaprasad − *Department of Engineering, Durham University,, Durham DH1 3LE, U.K.*

Antony Paul Roskilly − *Department of Engineering, Durham University,, Durham DH1 3LE, U.K.*

Complete contact information is available at: https://pubs.acs.org/10.1021/acs.energyfuels.0c01647

Notes

The authors declare no competing financial interest.

https://dx.doi.org/10.1021/acs.energyfuels.0c01647
Energy Fuels XXXX, XXX, XXX−XXX

■ ACKNOWLEDGMENTS

This project was funded through the EPSRC grant EP/R041970/2. Data supporting this publication is openly available under an 'Open Data Commons Open Database License'. Data underpinning this article can be found at doi:10.15128/r202870v911.

■ ABBREVIATIONS

Acronyms

aBDC = after bottom dead center
aTDC = after top dead center
EV = electric vehicle
EVO = exhaust valve opening
FPE = free-piston engine
FPEG = free-piston engine generator
FPLG = free-piston linear generator
ICE = internal combustion engine
iMEP = indicated mean effective pressure
IVC = intake valve closing
MEP = mean effective pressure
NVH = noise vibration and harshness

■ REFERENCES

(1) Mikalsen, R.; Roskilly, A. The design and simulation of a two-stroke free-piston compression ignition engine for electrical power generation. *Appl. Therm. Eng.* **2008**, *28*, 589−600.
(2) Mikalsen, R.; Roskilly, A. A review of free-piston engine history and applications. *Appl. Therm. Eng.* **2007**, *27*, 2339−2352.
(3) Jia, B.; Zuo, Z.; Tian, G.; Feng, H.; Roskilly, A. Development and validation of a free-piston engine generator numerical model. *Energy Convers. Manage.* **2015**, *91*, 333−341.
(4) Hanipah, M. R.; Mikalsen, R.; Roskilly, A. Recent commercial free-piston engine developments for automotive applications. *Appl. Therm. Eng.* **2015**, *75*, 493−503. http://www.sciencedirect.com/science/article/pii/S1359431114008114
(5) Jia, B.; Mikalsen, R.; Smallbone, A.; Roskilly, A. P. A study and comparison of frictional losses in free-piston engine and crankshaft engines. *Appl. Therm. Eng.* **2018**, *140*, 217−224.
(6) Yuan, C.; Feng, H.; He, Y.; Xu, J. Motion characteristics and mechanisms of a resonance starting process in a free-piston diesel engine generator. *Proc. Inst. Mech. Eng., Part A* **2016**, *230*, 206−218.
(7) Chiang, C.-J.; Yang, J.-L.; Lan, S.-Y.; Shei, T.-W.; Chiang, W.-S.; Chen, B.-L. Dynamic modeling of a si/hcci free-piston engine generator with electric mechanical valves. *Appl. Energy* **2013**, *102*, 336−346. Special Issue on Advances in sustainable biofuel production and use—XIX International Symposium on Alcohol Fuels—ISAF. http://www.sciencedirect.com/science/article/pii/S0306261912005557
(8) Li, Q.; Xiao, J.; Huang, Z. Simulation of a two-stroke free-piston engine for electrical power generation. *Energy Fuels* **2008**, *22*, 3443−3449.
(9) Feng, H.; Guo, C.; Yuan, C.; Guo, Y.; Zuo, Z.; Roskilly, A. P.; Jia, B. Research on combustion process of a free piston diesel linear generator. *Appl. Energy* **2016**, *161*, 395−403. http://www.sciencedirect.com/science/article/pii/S0306261915012969
(10) Kim, J.; Bae, C.; Kim, G. Simulation on the effect of the combustion parameters on the piston dynamics and engine performance using the wiebe function in a free piston engine. *Appl. Energy* **2013**, *107*, 446−455. http://www.sciencedirect.com/science/article/pii/S0306261913001748
(11) Kock, F.; Haag, J.; Friedrich, H. E. In *The Free Piston Linear Generator-Development of an Innovative, Compact, Highly Efficient Range-Extender Module*, No. 2013-01-1727; SAE Technical Paper, 2013.
(12) Haag, J.; Ferrari, C.; Starcke, J. H.; Stöhr, M.; Riedel, U. In *Numerical and Experimental Investigation of In-Cylinder Flow in a Loop-Scavenged Two-Stroke Free Piston Engine*, No. 2012−32−0114; SAE Technical Paper, 2013.
(13) Ferrari, C.; Friedrich, H. E. In *Development of a Free-Piston Linear Generator for Use in an Extended-Range Electric Vehicle*, Proceedings of the EVS26 International Battery Hybrid and Fuel Cell Electric Vehicle Symposium, Los Angeles, CA, USA, 2012; pp 6−9.
(14) Kock, F.; Heron, A.; Rinderknecht, F.; Friedrich, H. E. The free-piston linear generator potentials and challenges. *MTZ worldwide* **2013**, *74*, 38−43.
(15) Kosaka, H.; Akita, T.; Moriya, K.; Goto, S.; Hotta, Y.; Umeno, T.; Nakakita, K. In *Development of Free Piston Engine Linear Generator System Part 1-Investigation of Fundamental Characteristics*, No. 2014−01−1203, SAE Technical Paper, 2014.
(16) Goto, S.; Moriya, K.; Kosaka, H.; Akita, T.; Hotta, Y.; Umeno, T.; Nakakita, K. In *Development of Free Piston Engine Linear Generator System Part 2-Investigation of Control System for Generator*, No. 2014−01−1193, SAE Technical Paper, 2014.
(17) Moriya, K.; Goto, S.; Akita, T.; Kosaka, H.; Hotta, Y.; Nakakita, K. In *Development of Free Piston Engine Linear Generator System Part 3-Novel Control Method of Linear Generator for to Improve Efficiency and Stability*, No. 2016−01−0685, SAE Technical Paper, 2016.
(18) Nandkumar, S. Two-Stroke Linear Engine. Ph.D. Thesis, West Virginia University, 1998.
(19) Blarigan, P. V.; Paradiso, N.; Goldsborough, S. In *Homogeneous Charge Compression Ignition with a Free Piston: A New Approach to Ideal Otto Cycle Performance*, No. 982484, SAE Technical Paper, 1998.
(20) Goldsborough, S. S.; Blarigan, P. V. A numerical study of a free piston ic engine operating on homogeneous charge compression ignition combustion. *SAE Trans.* **1999**, 959−972.
(21) Xu, Z.; Chang, S. Prototype testing and analysis of a novel internal combustion linear generator integrated power system. *Appl. Energy* **2010**, *87*, 1342−1348.
(22) Jia, B.; Tian, G.; Feng, H.; Zuo, Z.; Roskilly, A. An experimental investigation into the starting process of free-piston engine generator. *Appl. Energy* **2015**, *157*, 798−804.
(23) Jia, B.; Zuo, Z.; Feng, H.; Tian, G.; Smallbone, A.; Roskilly, A. Effect of closed-loop controlled resonance based mechanism to start free piston engine generator: Simulation and test results. *Appl. Energy* **2016**, *164*, 532−539.
(24) Guo, C.; Feng, H.; Jia, B.; Zuo, Z.; Guo, Y.; Roskilly, T. Research on the operation characteristics of a free-piston linear generator: Numerical model and experimental results. *Energy Convers. Manage.* **2017**, *131*, 32−43.
(25) Feng, H.; Guo, C.; Yuan, C.; Guo, Y.; Zuo, Z.; Roskilly, A. P.; Jia, B. Research on combustion process of a free piston diesel linear generator. *Appl. Energy* **2016**, *161*, 395−403.
(26) Guo, C.; Song, Y.; Feng, H.; Zuo, Z.; Jia, B.; Zhang, Z.; Roskilly, A. Effect of fuel injection characteristics on the performance of a free-piston diesel engine linear generator: Cfd simulation and experimental results. *Energy Convers. Manage.* **2018**, *160*, 302−312.
(27) Kim, J.; Bae, C.; Kim, G. The operation characteristics of a liquefied petroleum gas (lpg) spark-ignition free piston engine. *Fuel* **2016**, *183*, 304−313.
(28) Zhang, C.; Sun, Z. Trajectory-based combustion control for renewable fuels in free piston engines. *Appl. Energy* **2017**, *187*, 72−83. http://www.sciencedirect.com/science/article/pii/S0306261916316300
(29) Virsik, R.; Heron, A. In *Free Piston Linear Generator in Comparison to Other Range-Extender Technologies*, 2013 World Electric Vehicle Symposium and Exhibition (EVS27), 2013; pp 1−7.
(30) Heron, A.; Rinderknecht, F. In *Comparison of Range Extender Technologies for Battery Electric Vehicles*, 2013 Eighth International Conference and Exhibition on Ecological Vehicles and Renewable Energies (EVER), 2013; pp 1−6.
(31) Raide, V.; Ilves, R.; Küüt, A.; Küüt, K.; Olt, J.; et al. Existing state of art of free-piston engines. *Agron. Res.* **2017**, *15*, 1204−1222.
(32) Wang, X.; Chen, F.; Zhu, R.; Yang, G.; Zhang, C. A review of the design and control of free-piston linear generator. *Energies* **2018**, *11*, No. 2179.

(33) Woo, Y.; Lee, Y. J. Free piston engine generator: Technology review and an experimental evaluation with hydrogen fuel. *Int. J. Autom. Technol.* **2014**, *15*, 229−235.
(34) Hung, N. B.; Lim, O. A review of free-piston linear engines. *Appl. Energy* **2016**, *178*, 78−97. http://www.sciencedirect.com/science/article/pii/S0306261916308133
(35) Rikard Mikalsen, A. P. R. Free-Piston Internal Combustion Engine. US Patent US201301184532013. https://patents.google.com/patent/US2013011845.3/it.
(36) Jia, B.; Wu, D.; Smallbone, A.; Ngwaka, U. C.; Roskilly, A. P. Dynamic and thermodynamic characteristics of a linear joule engine generator with different operating conditions. *Energy Convers. Manage.* **2018**, *173*, 375−382. http://www.sciencedirect.com/science/article/pii/S0196890418308392
(37) Caterpillar, Rp4400 Genset Specification, 2018. https://shop.cat.com/en/gbr/rp4400-501-5153.
(38) Honda, Em5500s Generator Specification, 2018. http://www.justhonda.co.uk/honda-em5500s-generator.html.
(39) Ford, Ecoboost Specification, 2018. https://www.ford.co.uk/content/dam/guxeu/uk/documents/home/experience-ford/about-ford/ford-component-sales/specification-details-data-sheets/20-ecoboost-np.pdf.
(40) Ford, Gti2.0 Specification, 2018. https://www.ford.co.uk/content/dam/guxeu/uk/documents/home/experience-ford/about-ford/ford-component-sales/specification-details-data-sheets/20-gdi-np.pdf.
(41) Lotus Fagor Specification, 2010. http://www.lotuscars.com/engineering/range-extender-engines.
(42) Turner, J.; Blake, D.; Moore, J.; Burke, P.; Pearson, R.; Patel, R.; Blundell, D.; Chandrashekar, R.; Matteucci, L.; Barker, P.; Card, C. The lotus range extender engine. *SAE Int. J. Engines* **2010**, *3*, 318−351.
(43) Mahle, Range Extender Specification, 2010. http://www.mahle-powertrain.com/C1257126002DFC22/vwContentByUNID/7BD528F92F833F5BC12578D1004AA089.
(44) Fraidl, G. K.; Beste, F.; Kapus, P. E.; Korman, M.; Sifferlinger, B.; Benda, V. In *Challenges and Solutions for Range Extenders—From Concept Considerations to Practical Experiences*, SAE Technical Paper, SAE International, 2011.
(45) Fischer, R.; Fraidl, G. K.; Hubmann, C.; Kapus, P. E.; Kunzemann, R.; Sifferlinger, B.; Beste, F. Range extender module. *ATZautotechnology* **2009**, *9*, 40−46.
(46) DOE Technical Targets for Fuel Cell Systems and Stacks for Transportation Applications, 2015. https://www.energy.gov/eere/fuelcells/doe-technical-targets-fuel-cell-systems-and-stacks-transportation-applications.
(47) Tube, N. U. Y. Free-Piston Engine Range Extender Technology, 2016. https://www.youtube.com/watch?v=u4b0_6byuFU.
(48) Hanipah, M. R. Development of a Spark Ignition Free-Piston Engine Generator. Ph.D. Thesis, Newcastle University, 2015. http://hdl.handle.net/10443/2881.
(49) Ngwaka, U.; Smallbone, A.; Jia, B.; Lawrence, C.; Towell, B.; Roy, S.; KV, S.; Roskilly, A. P. Evaluation of performance characteristics of a novel hydrogen-fuelled free-piston engine generator. *Int. J. Hydrogen Energy* **2020**, No. 72.
(50) Heywood, J. *Internal Combustion Engine Fundamentals*; McGraw-Hill, 1988.

https://dx.doi.org/10.1021/acs.energyfuels.0c01647
Energy Fuels XXXX, XXX, XXX−XXX